Efficient and Selective Recovery of Trace Scandium by Inorganic Titanium Phosphate Ion-Exchangers from Leachates of Waste Bauxite Residue

Zhang, Wenzhong

2017-02-20

Zhang , W , Koivula , R , Wiikinkoski , E , Xu , J , Hietala , S , Lehto , J & Harjula
Efficient and Selective Recovery of Trace Scandium by Inorganic Titanium Phosphate
Ion-Exchangers from Leachates of Waste Bauxite Residue ' , ACS Sustainable Chemistry &
Engineering , vol. 5 , no. 4 , pp. 3103-3114 . https://doi.org/10.1021/acssuschemeng.6

http://hdl.handle.net/10138/179107
https://doi.org/10.1021/acssuschemeng.6b02870

submittedVersion

Efficient and Selective Recovery of Trace Scandium by Inorganic Titanium Phosphate Ion-Exchangers from Leachates of Waste Bauxite Residue

Wenzhong Zhang*

The high Sc^{3+} selectivity by amorphous TiP was suspected to be the matching of Ti^{4+} lattice radius with Sc^{3+} ionic radius (both 0.745 Å). Finally, the separation of trace scandium from the simulated BR leachate solution was demonstrated on an amorphous TiP column. The interference of Fe^{3+} has been partially resolved by on-column reduction using sodium sulphite. The optimized final eluate contained only Sc, Fe and Al. The concentration ratio of Sc/Fe can be increased by a factor of 8.8 and Sc/Al by 265 through a single cycle of chromatographic separation with a Sc recovery rate of 91.1%.

KEYWORDS

Titanium phosphate; scandium recovery; ion exchange; bauxite residue.

LIST OF ABBREVIATIONS

Amorphous titanium phosphate (am-TiP)

Bauxite residue (BR)

Field emission scanning electron microscopy (FE-SEM)

Fourier transformed infrared spectroscopy (FTIR)

Ion exchange capacity (IEC)

Magic-angle spinning nuclear magnetic resonance (MAS NMR)

Microwave plasma-atomic emission spectrometry (MP-AES)

Rare earth element (REE)

Separation factor (SF)

Thermogravimetric analysis (TGA)

Titanium phosphate (TiP)

X-ray diffraction (XRD)

INTRODUCTION

Rare earth elements (REEs) play an increasingly vital role in modern material technology owing to their unique characteristics.[1] Among all the REEs, scandium is exceptionally rare and expensive.[2] On the supply side, it is not an unabundant element but is distributed in trace amounts alongside other mineral ores. It is only produced as a by-product of other metal production.[3] On the consumer side, growing commercial application demands, including aluminium–scandium alloys,[4] solid oxide fuel cells,[5] etc., are now evidently inhibited by its low availability and high price.[6] Consequently, finding an additional route to manufacture the REEs from secondary resources has become a research hotspot.[7]

Bauxite residue (BR, red mud) is continuously produced as an industrial waste in large quantities during the extraction of alumina from bauxite ores through the Bayer process. An estimated worldwide BR inventory of 4 billion tonnes in 2015 constitutes the legacy of more than 100 years of alumina production.[8] However, its disposal remains a complicated task due to the extreme alkalinity (pH 10–13) and sodicity.[9] Historically, marine disposal, lagooning and dry stacking have been used, yet none of them has proven to be ideal.[10] There is thus a need to investigate large-volume and economically viable utilization options.[8] Typically, BR contains significant amounts of iron (hematite), silica (desilication product), calcium, aluminium (diaspore, boehmite and gibbsite) and titanium (rutile and perovskite) oxide minerals.[11] Extensive efforts have already been directed to the recovery of these major elements[8,12–14] as well as utilizing the remains for cement application.[15] Ores with a scandium content of 20–50 g t^{-1} are considered a scandium resource and deserve full exploitation, whereas the scandium concentration in some BR could reach 60–120 g t^{-1}.[16]

Considering the vast amount of BR generated, the extraction of REEs, especially scandium, potentially adds value to the whole valorisation chain. The complete conceptual separation process

for Sc from BR is illustrated in **Scheme S1**. To enable the extraction of REEs, they must be leached from BR. In a typical leaching process, BR is treated with mineral acid solutions to dissolve the REEs.[17, 18] Inevitably, excess amount of sodium, calcium, aluminium, silica, titanium and iron ions are co-leached with REEs into the leachate. The silica and titanium contents can be easily precipitated by addition of base without sacrificing the REEs. The recovery of highly diluted REEs (several ppm) from the acid BR leachate with high salt background (Na, Ca, Fe, Al at thousands of ppm) is still particularly challenging because of the selectivity requirements. Ion exchange and solvent extraction are two important processes for scandium recovery.[19] Previously, ionic liquids,[20] functionalized chitosan-silica bio-hybrid materials[21] and activated carbons[22] have been used for scandium recovery.

Inorganic ion exchangers with unique ion selectivity are a promising class of materials to this end. Insoluble acid salts of tetravalent metals have long been known for and extensively studied for their ion exchange behaviour. The presence of two types of functional groups, metal-OH and phosphoric acid groups, enables the material to exhibit amphoteric behavior.[23] The protons within the phosphate groups are predominantly responsible for ion exchange capability. Titanium phosphate (TiP) materials were chosen for the current study as these materials have great acid stability enabling their use in the acid leaching solution. The oxygens in the PO_4^{3-} tetrahedron can be shared in different ways with titanium in an octahedral configuration, giving rise to altered structural combinations such as amorphous, fibrous, layered or three-dimensional structures.[24-26] Among these, the most investigated are amorphous TiP and lamellar-

exhibits an excellent host structure for post-synthesis modification of the interlayer space.[29] Chromatographic separation of inorganic ions has been achieved on crystalline TiP thin layers.[30] To date, the ion exchange behaviour of TiP or similarly zirconium phosphate, has been systematically reported by Clearfield and Alberti.[24,31] In addition, mesoporous[32] and inorganic-organic composite[33, 34] TiP materials have been developed. However, little is known about their behaviour towards REE ions.

The aim of our work was to investigate the potential applicability of TiP ion exchangers in the separation of trace scandium/REEs from complex waste streams. This paper involves the synthesis of

(>99.9%) and scandium oxide (>99.99%) were acquired from Alfa Aesar (Helsinki, Finland). Cerium (III) chloride heptahydrate (>98.0%) was purchased from Fluka (Vienna, Austria). Orthophosphoric acid (85%) was obtained from VWR Chemicals (Helsinki, Finland). Sulfuric acid (95–97%) was purchased from J.T. Baker (Pennsylvania, US). Calcium nitrate tetrahydrate, sodium sulphite heptahydrate, and aluminium nitrate nonahydrate were obtained from Riedel-de Haen GmbH (Seelze, Germany). All elemental (Al, Ca, Ce, Dy, Fe, La, Na, Nd, Sc, and Ti) single standard solutions (1000 mg L^{-1}, PrimAg–plus cert. ref. material) and nitric acid (SpA super purity, 67–69%) were purchased from Romil (Cambridge, UK). Milli-Q water (Millipore) with the resistivity of 18.2 M

180 °C for 12 h. The product was filtered, washed with water until a pH of 3.5 were reached and then air-dried at 70 °C.

Synthesis of

performed by OriginPro 8.6 using 100% Lorentzian peak. TGA was performed using a Mettler Toledo TGA/DSC 1 instrument under nitrogen atmosphere,

where

concentration have limited effect on the ion exchange of multivalent elements because of its low ability to form a

Two systems of initial loading solution were studied: 1 mM Sc and 1 mM equimolar mixture of Ca, Al and Fe (III). The K_d (mg L^{-1}) values of the elution systems were calculated as follows:

Al at pH 4.0. The elution was done by 20 mL of 0.5 M equimolar mixture of nitric acid and phosphoric acid. Altogether five cycles were performed. The Sc uptake and $SF_{(Sc/Al)}$ in each cycle were calculated.

RESULTS AND DISCUSSION

Characteristics of TiPs. Three types of synthesized TiPs were characterized using chemical analysis, XRD, FE-SEM, FTIR, UV/Vis diffuse reflectance spectrometry, solid state ^{31}P MAS NMR, TGA and potentiometric titration. Chemical analysis showed that the molar PO_4/Ti ratios are 1.02 ± 0.01, 1.97 ± 0.04 and 1.98 ± 0.03 for am-

and asymmetrical stretching vibration of PO_3^-.[36,41] Different modes of free surface

Upon heating in an inert atmosphere, dehydration and dehydroylation reactions occur within the TiP materials (**Fig. 4**). The free water and crystal water are lost in the initial stage, and under higher temperature the hydroxyl condensation occurs, leading to the formation of pyrophosphate. In the case of am-TiP, all these processes are overlapped considerably and some of them occur simultaneously.[23] To obtain the formula of am-TiP and understand its pyrolytic process, additional studies were performed. The sulphate ion uptake capacity of the am-TiP was determined to be 3.17 meq g^{-1} in 0.05 M H_2SO_4-Na_2SO_4 system. The XRD pattern (**Fig. S3**) of the am-TiP treated at 1000 °C shows only pyrophosphate $Ti_2O(PO_4)_2$ or $(TiO)_2P_2O_7$ phase without any TiO_2 present. The two pyrophosphate isomers are indistinguishable by XRD. It is known that $Ti_2O(PO_4)_2$ transforms to $(TiO)_2P_2O_7$ phases at 700 to 1000 °C with no weight loss.[26] Combined with the Ti and P contents obtained from chemical analysis (correspondingly 25.36% and 16.73%), the composition of our am-TiP was identified as $TiO_{1.11}(OH)_{0.58}(HPO_4)_{0.2}(H_2PO_4)_{0.8}\cdot 0.64H_2O$, which is a hydrous titanium oxohydroxyphosphate material. Its overall thermal decomposition with theoretical weight loss of 17.94% can be expressed by the following equation:

Potentiometric titration (both with and without salt addition) was performed to confirm the existence states of phosphate groups (**Fig. 5**) and the total ion exchange capacity (IEC) of the TiPs were determined by titration without added salt and by measuring Na^+ uptake. The total IEC corresponds to the amount of Na^+ ions added before reaching the plateau in the titration curves (without salt addition).[45] The am-TiP exhibited steadily increasing titration curve, thereby confirming its amorphous nature. It is noted that in the titration curve of am-TiP without added salt, one inflection point at pH 4 can be observed, probably due to the first proton dissociation from H_2PO_4 or HPO_4 group. The total IEC estimated by titration curve is 5.6 meq g^{-1}, while the same by Na_2CO_3 sorption equals to 5.13 meq g^{-1}. The Na^+ IEC account for 52.4-57.2% of its total formula-calculated IEC (9.79 meq g^{-1}). The titration curves of the layered TiPs showed single- and di-protonic behaviour with clearly visible pH plateaus and inflection points between them. The pK_a values were chosen from the midpoint of the pH plateaus. Titration without added salt gives directly the pK_a values, and for titration with 0.1 M $NaNO_3$ background, the pK_a values are only apparent values. The apparent pK_a values cannot be directly compared with the pK_a values of dissolved phosphoric acids because the former is strongly dependent on the added salt concentration in the titration system.[46] The IECs and chemical formulae of the TiPs are summarized in **Table 1**. The Na^+ IEC from batch sorption of Na_2CO_3 solution agreed well with the titration data of both approaches. The pK_a values of layered TiPs could

of the titration. The p*K*a values

of increased polymerized tetravalent $Sc_2(OH)_2^{4+}$ and decreased divalent $Sc(OH)^{2+}$ concentration resulted in the virtually unchanged uptake capacity from pH 3 to 4.

Separation factors in binary equimolar mixtures. Excess amounts of major metal ions, namely Al^{3+}, Fe^{3+}, Ca^{2+}, Si^{4+}, Ti^{4+} and Na^{+}, are present in the acid BR leaching solution. Ti^{4+} and Si^{4+} do not cause much trouble since they can be easily precipitated at around pH 2 without sacrificing the Sc and REE content. Monovalent and divalent ions have lower affinity towards the TiPs than trivalent Sc^{3+} and are therefore tolerable even at very high concentrations (thousands of ppm).[39] The biggest challenge for separation of Sc^{3+} arises from the trivalent ions, especially Fe^{3+}, which shares chemical similarities with Sc^{3+}.[21] The elimination of Fe^{3+} is not possible through precipitation due to the occurrence of scandium co-precipitation. Notably, one approach for eliminating the interference of Fe^{3+} is to reduce it to Fe^{2+}. Direct reduction of Fe^{3+} in the leaching solution is not possible in an economically viable and eco-friendly manner. In this paper, on-column reduction of Fe^{3+} was used for efficient separation of Fe^{3+} and Sc^{3+}, as will be later seen. Herein, the divalent iron as a competing ion for Sc^{3+}, instead of the trivalent one, was studied as it gave more flexibility for pH adjustment (< pH 3.5) compare to Fe^{3+} (< pH 2). **Fig. S4** (*a*, *b* and *c*) illustrates the behaviour of SF between Sc and individually Al, Ca, Fe, Y with equilibrium pH on three TiPs. Notably, am-TiP gave the highest SF in all cases. At around pH 2, all of the SFs calculated were over 10, with $SF_{(Sc/Al)}$ and $SF_{(Sc/Y)}$ higher than 1000 and $SF_{(Sc/Fe2+)}$ around 80 on am-TiP. The results of high SFs indicated that am-TiP might be a promising material for the separation of Sc^{3+} from all other elements present in the BR leachate. However, layered crystalline materials showed considerably lower SFs in the order of 1 to 10 throughout the tested pH range.

Ion exchange capacity and stoichiometry. The Sc^{3+} ion exchange isotherms were determined at around pH 2.0 for all three TiPs (**Fig. 7**, *a*). The IECs read from the isotherms are 1.74, 0.55 and 0.22

meq g^{-1} foram –

mechanism of ion selectivity by TiP materials, the solubility product constants (K_{sp}) of different metal phosphates were compared. According to the literature,[51-53] the order of solubility (mol L^{-1}) for four metal phosphates is as follows: $S(FePO_4)=1.8\times10^{-17} < S(AlPO_4)=10^{-16} < S(ScPO_4)=3.2\times10^{-9} < S[Ca_3(PO_4)_2]=4.2\times10^{-6}$. The order of iron, aluminium and calcium are in line with their selectivity by the material. Contrary to our understanding, scandium, with the second highest solubility of its phosphate, is the most selected ion by TiP materials. Therefore, other factors might provide a dominating effect for scandium selectivity. **Table 3** summarizes some important factors regarding the ions available in BR leachate.[54-61] Ion exchange material can compete with the hydration of ions. In TiPs, Ti atoms are coordinated by phosphate groups in an octahedral manner. The ion exchange behaviour arises from protons of phosphate groups and also via the coordination bond with the phosphoryl group. Our proposed theory is that TiP might favour ions that share a similar radius with the structural forming Ti. According to Shannon,[54] the lattice radius of octahedrally coordinated Ti^{4+} is

Our observation from related XRD data indicated that the interlayer distance remained the same after Sc^{3+} aqua ion exchange, which might limit the capacity and selectivity. Further structural investigations are needed to validate the explanation. Based on the proposed mechanism, it is also possible that other kinds of am-TiP materials have high selectivity towards Sc^{3+}.

Batch elution tests. Batch elution studies were conducted to provide basic information for later column elution such as prerequisites for the choice of acids and concentrations. Due to am-TiP having the highest capacity and selectivity towards Sc^{3+}, only elution on am-TiP was investigated in this study. The first system studied was elution of Sc^{3+} from Sc-loaded am-TiP. The results in **Fig. 8** (*a*) show that the elution K_d values of Sc decreased with increasing acid concentration. Under the same molarity, the elution efficiency followed the sequence of $H_2SO_4 > H_3PO_4 > HNO_3$. Over 90% of the elution efficiency could be achieved using 1 M HNO_3. The material stability was also assessed here by repeated elution using 1 M HNO_3, and the corresponding Ti and P hydrolysis fractions for three consecutive cycles were 0.5%, 1.5% and 1.8% for Ti and 0.4%, 1.2% and 1.6% for P. The hydrolysed Ti would not interfere with the Sc recovery since it could be precipitated easily, and the hydrolysed phosphate only constitutes as minor background salt. Another system studied here was the elution of metal-loaded TiP from an equimolar ternary mixture of Fe^{2+}, Ca and Al. **Fig. 8** (*b*) illustrates the elution K_d values in this system. The K_d values of Fe^{2+} dropped with increasing in acid concentration, and the elution efficiency of acids followed the same order ($H_2SO_4 > H_3PO_4 > HNO_3$) as with scandium. For Ca^{2+} and Al^{3+}, by contrast, the K_d values almost remained unchanged or changed only slightly. This levelling phenomenon is probably because Fe^{2+} binds most strongly with am-TiP material, and therefore, increasing acid concentration only affected the elution of Fe^{2+}. Taking advantage of this phenomenon

could lead to the elution of weakly binding ions at lower acid concentration, followed by firmly binding ions (including Sc^{3+}) at higher acid concentration.

Chromatographic separation of Sc^{3+} from simulated BR leachate. The simulated BR leachate at pH 1.5 was prepared according to the composition reported by Roosen.[21] This specific composition originated from a Greek BR. Tetravalent ions were first removed from the leachate by means of alkaline precipitation. By adjusting the pH from 1.5 to 2.0 with NaOH, almost all Si^{4+} and Ti^{4+} were removed (**Table 3**), with only 2.5% of Sc^{3+} loss. Therefore, Si^{4+} and Ti^{4+} were not considered in further separation. The resulting solution was loaded onto an am-TiP column to study the breakthrough behaviour. As illustrated in **Fig. 9** (*a*), Na^{+}, Al^{3+}, Ca^{2+} and La^{3+} broke through the column before 5 BV. Fe^{3+} started to breakthrough at 18 BV and Sc^{3+} at 22 BV. This further confirmed the similarity between trivalent iron and scandium. In a further test, to achieve better separation, ca. 8 BV of the simulant was loaded onto the am-TiP column, and on-column reduction of Fe^{3+} was performed by conditioning the column with 2 BV of 0.05 M sodium sulphite. The reducing agent employed here can be recycled to lower its consumption. The elution chromatogram for this run is presented in **Fig. 9** (*b*) by means of cumulative elution percentage versus bed volume. With 0.2 M nitric acid, the majority of Fe (including Fe^{2+} and Fe^{3+}) and Al^{3+} as well as all of the Na^{+}, La^{3+} and Ca^{2+} eluted from the column. After this, 0.3 M nitric acid further eluted some Fe and Al^{3+}, however, Sc^{3+} also started to come out of the column. By elution with a mixed acid comprising 0.5 M nitric and 0.5 M phosphoric acid, all (98.9%) Sc^{3+} contents eluted. Combining the final 30 BV of eluent, we obtained a solution containing only Sc^{3+}, Fe and Al^{3+} at concentrations of 0.35, 1.43 and 0.28 ppm, respectively, while in the original feed solution, the corresponding Sc^{3+}, Fe^{3+} and Al^{3+} concentrations were 1.96, 72.3 and 636 ppm. The concentration ratio of Sc/Fe increased from 1/35 to 1/4 and Sc/Al from 1/318 to 1/1.2 through a single cycle of

chromatographic separation. The on-column reduction conditions and other elution agents are now being further studied to achieve full reduction and better separation.

Reusability of am-TiP. The am-TiP underwent five cycles of sorption and elution to investigate its reusability. The equilibrium pH of the five sorption cycles were measure to be 2.1 ± 0.1. As illustrated in Fig. S5, slight decrease of Sc uptake was observed. However, the $SF_{Sc/Al}$ stayed on a relatively constant level under the logarithmic scale. The results indicate good reusability of the material.

CONCLUSION

TiP materials exhibit excellent host structures for the separation of trace scandium from complex BR acid leachate. Amorphous TiP has the highest scandium selectivity among the three TiPs tested. The unique selectivity towards Sc^{3+} is assumed to originate from the matching between the lattice radius of Ti^{4+} and the ionic radius of Sc^{3+}. The optimum separation pH was chosen at 2.0 for both capacity and selectivity considerations. The biggest challenges in the separation of Sc^{3+} from BR leachate are the interference from Fe^{3+} and Al^{3+}. By employing on-column reduction, Fe^{3+} was partially converted to less-favoured Fe^{2+} and the amount of reductant needed was minimized. All sodium, calcium and lanthanides and the majority of iron and aluminium were eluted from the column by 0.2 M nitric acid. Almost all scandium was then eluted by a mixed acid comprising nitric and phosphoric acid, with Sc/Fe and Sc/Al enrichment factors at 9 and 265, respectively. A pure scandium fraction is expected to be obtained by tandem chromatographic separations utilizing am-TiP. Overall, the TiP materials showed promising applicability for trace scandium recovery from complex waste streams.

ACKNOWLEDGEMENTS

The research leading to these results has received funding from the European Comm

REFERENCES

1. Massari, S.; Ruberti, M. Rare earth elements as critical raw materials: Focus on international markets and future strategies. *Resour. Policy*, 2013, 38, 36–43. (doi: 10.1016/j.resourpol.2012.07.001)
2. Baba, Y.; Fukami, A.; Kubota, F.; Kamiya, N.; Goto, M. Selective extraction of scandium from yttrium and lanthanides with amic acid-type extractant containing alkylamide and glycine moieties. *RSC Adv.*, 2014, 4, 50726–50730. (doi: 10.1039/C4RA08897B)
3. Wang, W.; Pranolo, Y.; Cheng, C.Y. Metallurgical processes for scandium recovery from various resources: A review. *Hydrometallurgy*, 2011, 108, 100–108. (doi: 10.1016/j.hydromet.2011.03.001)
4. Jindal, V.; De, P.K.; Venkateswarlu, Effect of Al$_3$Sc precipitates on the work hardening behavior of aluminum

(doi:10.1016/j.jhazmat.2011.03.004)
15. Pontikes, Y.; Angelopoulos, G.N. Bauxite residue in cement and cementitious applications: Current status and a possible way forward. *Resour. Conserv. Recy.*, 2013, 73, 53-63. (doi:10.1016/j.resconrec.2013.01.005)
16. Shaoquan, X.; Suqing, L. Review of the extractive metallurgy of scandium in China (1978

29. Clearfield, A.; Roberts, B.D. Pillaring of layered zirconium and titanium phosphates. *Inorg. Chem.*, 1988, 27, 3237–3240.
(doi:10.1021/ic00291a040)
30. Alberti, G.; Giammari, G.; Grassini-Strazza, G. Chromatographic behaviour of inorganic ions on crystalline titanium phosphate or zirconium phosphate thin layers. *J. Chromatogr. A*, 1967, 28, 118–123.
(doi:10.1016/S0021-9673(01)85936-7)
31. Clearfield, A. Recent advances in metal phosphonate chemistry. *Curr. Opin. Solid St. M.*, 1996, 1, 268–278.
(doi:10.1016/S1359-0286(96)80094-5)
32. Zhu, Y.-P.; Ren, T.-Z.; Yuan, Z.-Y. Insights into mesoporous metal phosphonate hybrid materials for catalysis. *Catal. Sci. Technol.*, 2015, 5, 4258–4279.
(doi:10.1039/C5CY00107B)
33. Zhu, Y.; Yoneda, K.; Kanamori, K.; Takeda, K.; Kiyomura, T.; Kurata, H.; Nakanishi, K. Hierarchically porous titanium phosphate monoliths and their crystallization behavior in ethylene glycol. *New J. Chem.*, 2016, 40, 4153–4159.
(doi:10.1039/C5NJ02820E)
34. Baig, U.; Rao, R.A.K.; Khan, A.A.; Sanagi, M.M.; Gondal, M.A. Removal of carcinogenic hexavalent chromium from aqueous solutions using newly synthesized and characterized polypyrrole

43. Garcia-Granda, S.; Khainakov, S.A.; Espina, A.; Garcia, J.R. Revisiting the thermal decomposition of layered

58. Persson, L.; D'Angelo, P.; De Panfilis, S.; Sandström, M.; Eriksson, L. Hydration of Lanthanoid (III) Ions in Aqueous Solution and Crystalline Hydrates Studied by EXAFS Spectroscopy and Crystallography: The

TABLES AND FIGURES

Table 1. Summary of chemical formulae and ion exchange capacities for TiPs.

Material	Formula	Theoretical IEC [a] (meq g^{-1})	Sorption Na^+ IEC (meq g^{-1}) [b]	Titration Na^+ IEC (meq g^{-1}) [c]	pK_{a1} [c]	pK_{a2} [c]	Apparent [d] pK_{a1}	Apparent [d] pK_{a2}
am-TiP	$TiO_{1.11}(OH)_{0.58}(HPO_4)_{0.2}(H_2PO_4)_{0.8}\cdot 0.64H_2O$	9.79	5.13	5.6	–	–	–	–

Table 2. Ion exchange characteristics of various am-TiP materials reported in literature.

Formula	Ti source	P:Ti molar ratio in mother liquid	Theoretical IEC (meq g^{-1})	Experimental IEC by Na^+ (meq g^{-1})	Reference
$Ti_4O_2(OH)_4(HPO_4)_3(H_2PO_4)_2 \cdot 3H_2O$	$TiCl_4$	3:1	8.46*	3.66	[48]
$TiO_{1.25}(OH)_{0.47}(HPO_4)_{0.13}(H_2PO_4)_{0.77} \cdot 2.3H_2O$	$TiCl_4$	2:1	8.2	4.7 (K^+)	[23]
$Ti(OH)_{1.36}(HPO_4)_{1.32} \cdot 2.3H_2O$	$TiOSO_4$	2:1	5.7	N.A.	[49]
$Ti(OH)_{1.2}(HPO_4)_{1.28}(H_2PO_4)_{0.24} \cdot 2.5H_2O$	$TiOSO_4$	2:1	6.78	5.56	[50]
$TiO(OH)(H_2PO_4) \cdot H_2O$	$TiOSO_4$	2:1	10.2*	6.30	[26]
$TiO_{1.11}(OH)_{0.58}(HPO_4)_{0.2}(H_2PO_4)_{0.8} \cdot 0.64H_2O$	$TiCl_4$	3.85:1	9.79	5.13	This work

** our calculation based on the given formulae.*

Table 3. Electron configuration, classical ionic radius, coordination number and metal-oxygen bond length of the ions present in BR leachate.

Ion	Electron configuration	Shannon ionic radius (Å) [54]	Coordination number	M-O bond length (Å)
Al^{3+}	[Ne]	0.535	6*	1.96 [55]
Ca^{2+}	[Ar]	1.12	8*	2.46 [56]
		1.00	6	–
Fe^{2+}	[Ar]$3d^6$	0.78	6*	2.118 [57]
Fe^{3+}	[Ar]$3d^5$	0.645	6*	1.994 [57]
Ln^{3+}	[Xe]$4f^0$-$4f^{14}$	La^{3+} 1.216 (max)	9*	La^{3+} 2.55 (max) [58]
		Lu^{3+} 1.032 (min)		Lu^{3+} 2.36 (min)
		La^{3+} 1.032 (max)	6	–
		Lu^{3+} 0.861 (min)		
Na^{+}	[Ne]	1.02	6*	2.42 [59]
Sc^{3+}	[Ar]	0.870	8	2.17 [60]
		0.745	6*	–
Y^{3+}	[Kr]	1.019	8*	2.37 [61]
		0.90	6	–
Ti^{4+}	[Ar]	0.605	6	–

Note: The number of water molecules coordinated in the metal aqua ions are marked with asterisks.

Table 3. Elemental composition (ppm) of simulated BR leaching solution at pH 1.5 and after pH adjustment to 2.0 and filtration.

Element	Na	Ca	Al	Fe	Si	Ti	Sc	La
BR leachate pH 1.5	1216	1069	641	94.3	572	95.7	2.01	5.30
BR leachate pH 2.0	2232	1037	636	72.3	0.1	3.1	1.96	5.24

Figure 1. Powder XRD patterns of the as-synthesized am –

Figure 2. FE-SEM micrographs of am-TiP (*a* and *b*

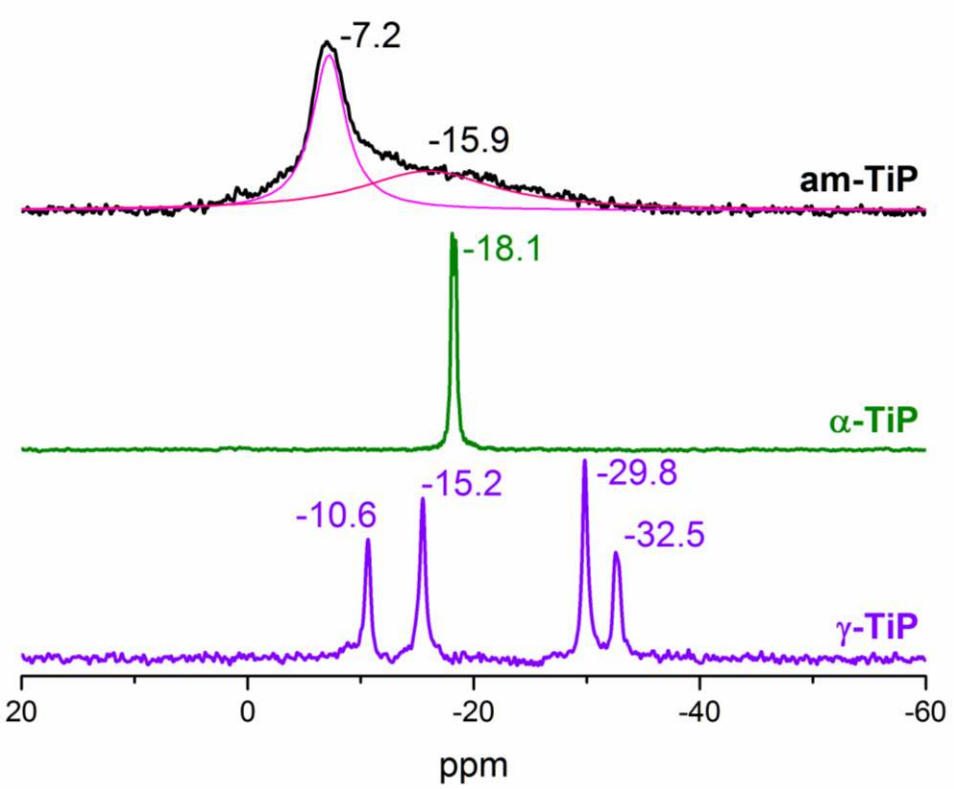

Figure 3. ^{31}P MAS NMR spectra of the TiPs. The line deconvolution was performed on the resonance peak of am-TiP.

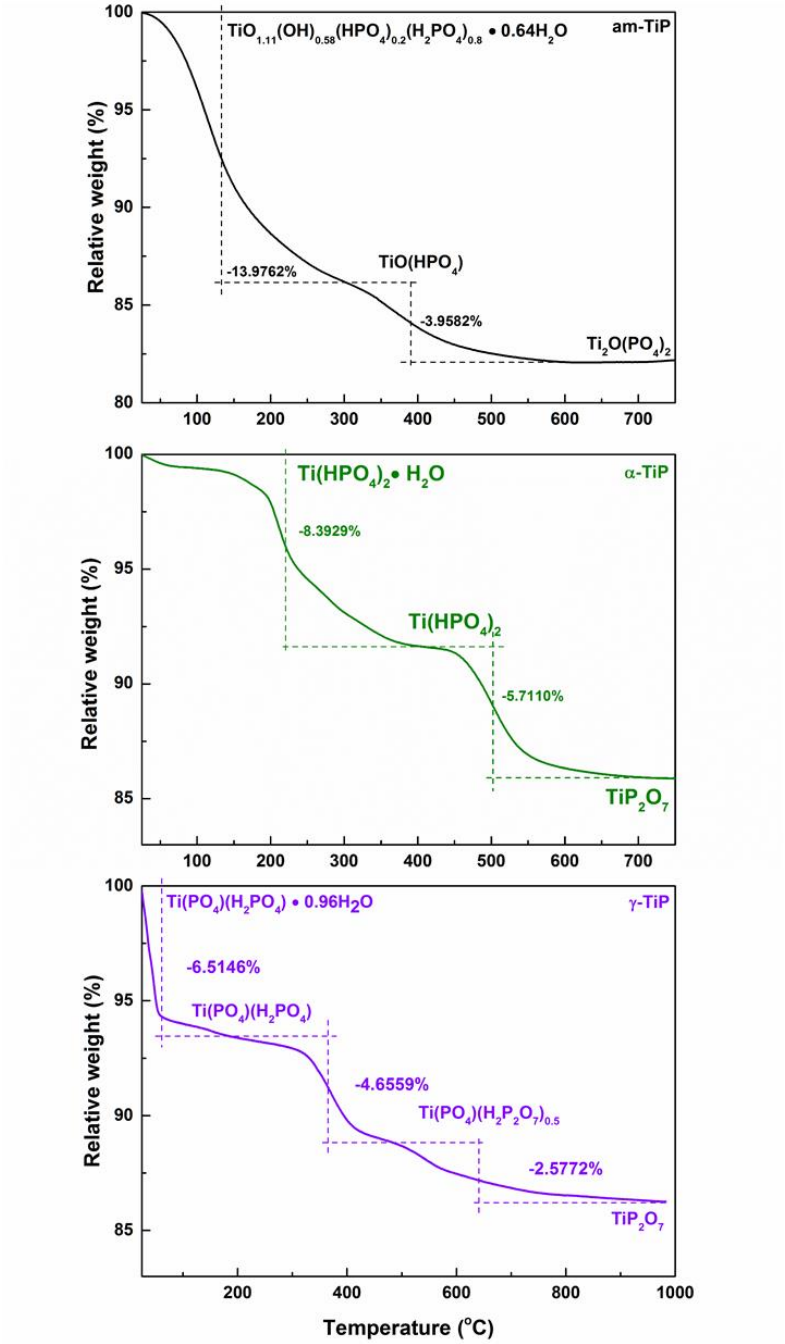

Figure 4. Thermograms of the TiP materials under nitrogen atmosphere at a heating rate of 10 °C min^{-1}. Weight loss stages were derived from first order differential TG curves.

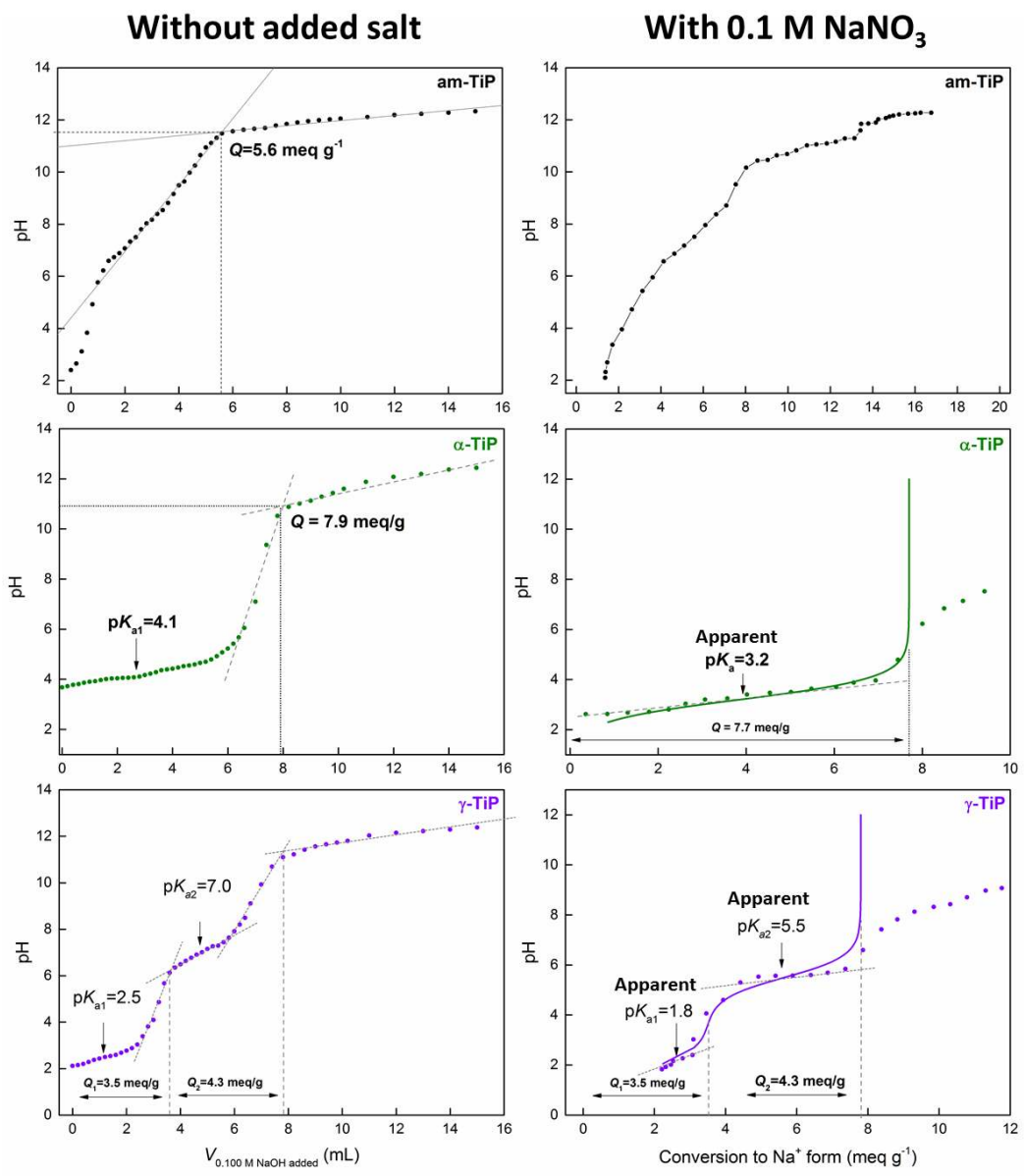

Figure 5. Potentiometric titration curves of the TiPs with (right column) and without added salts (left column). The titration curves (with added salt)

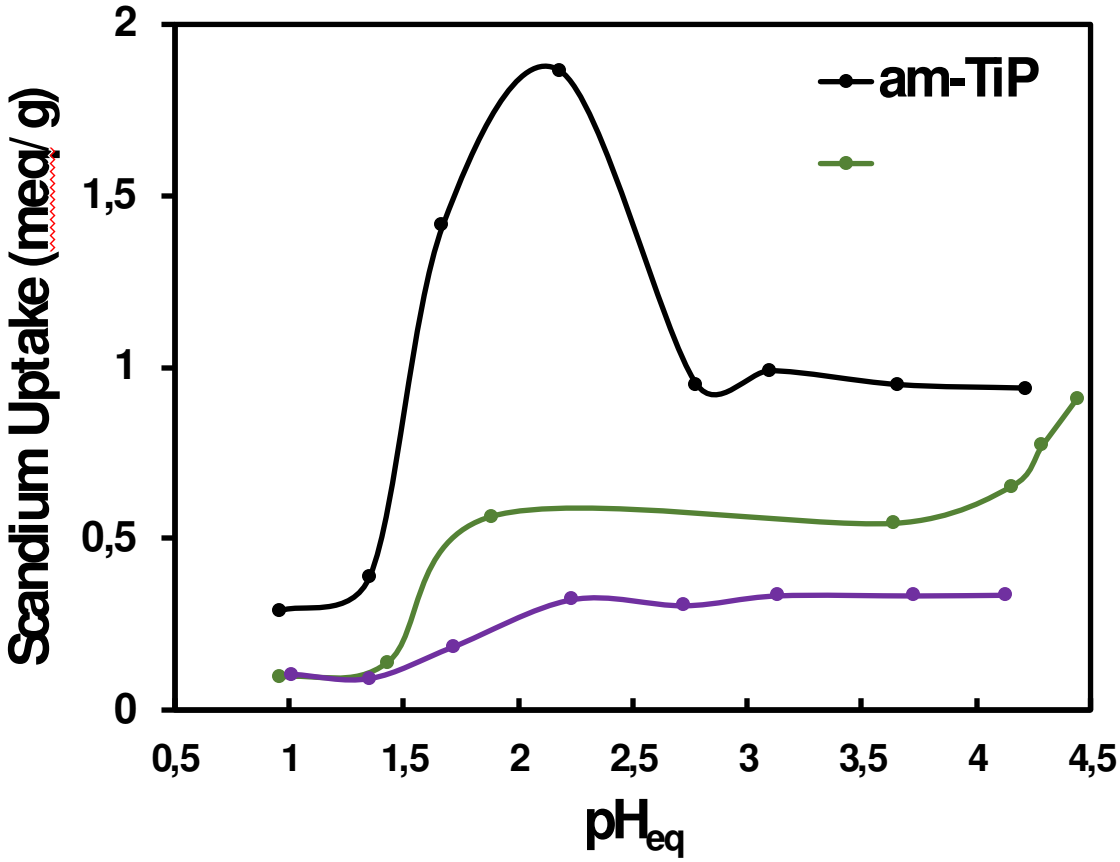

Figure 6. Effects of solution equilibrium pH on Sc uptakes of the TiP materials.

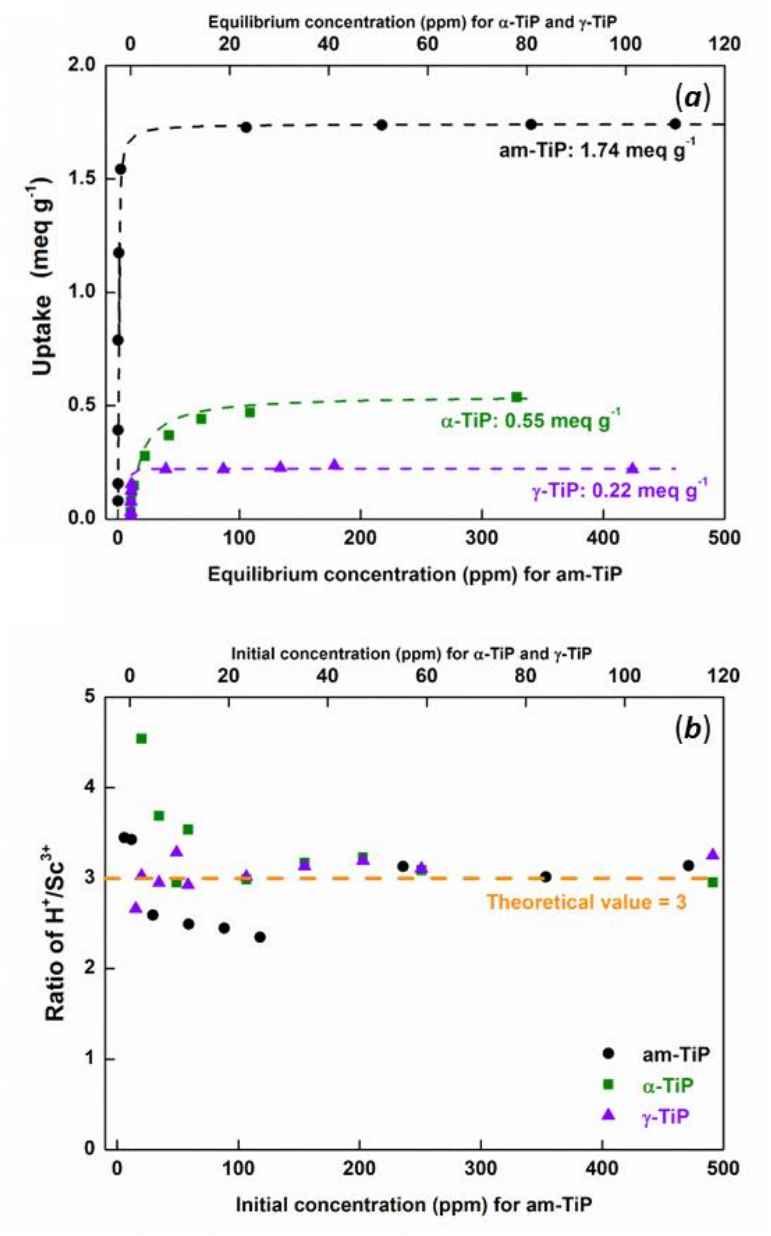

Figure 7. (*a*) Sc^{3+} ion exchange isotherms (25 °C) of the TiP materials at equilibrium pH 2.0 (±0.3) and capacities and (*b*) the corresponding ratios of H^+ released to Sc^{3+} adsorbed (H^+/Sc^{3+}) as a function of initial Sc^{3+} concentration.

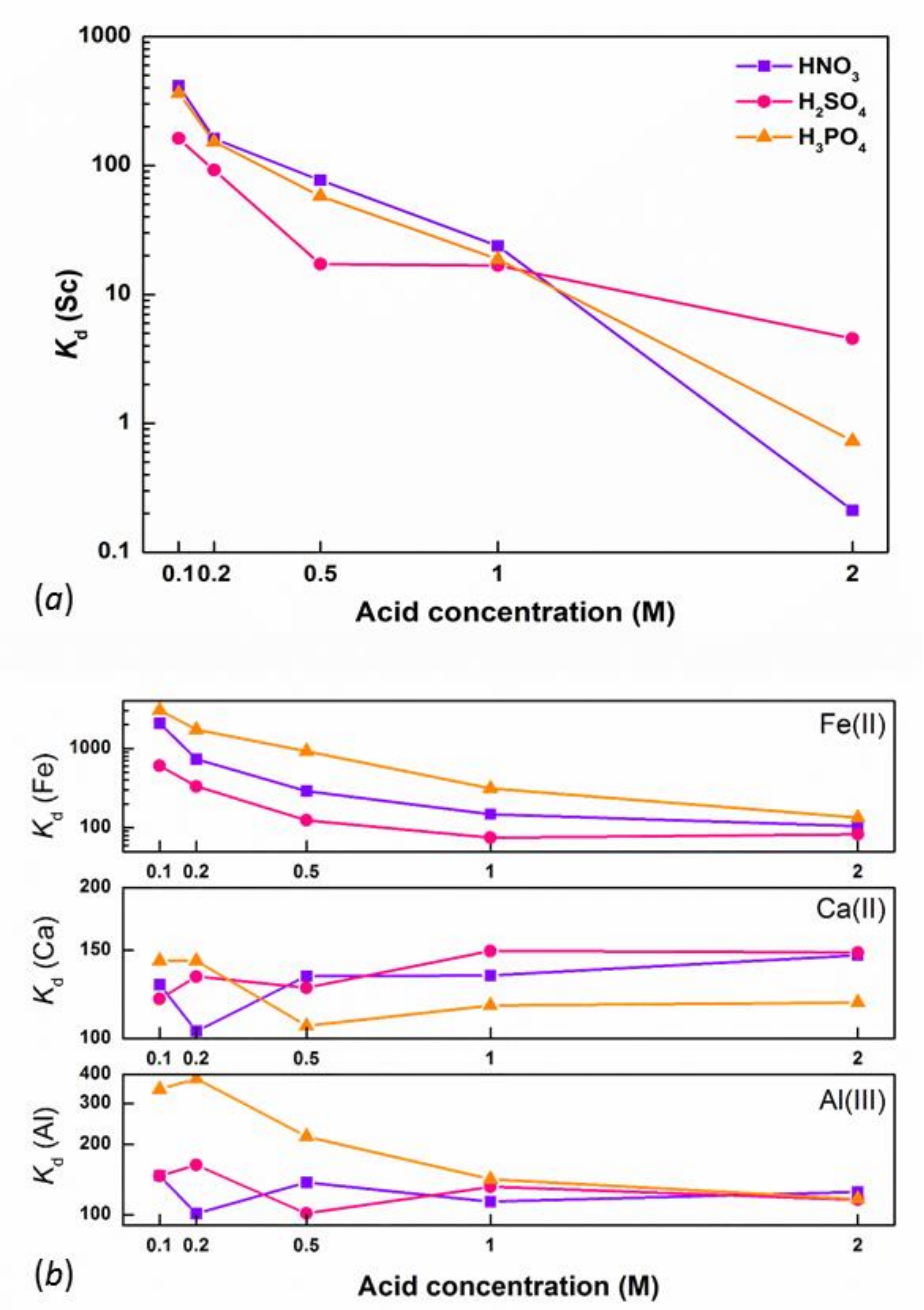

Figure 8. Effects of acid type and concentration on the distribution coefficients (K_d, mL g^{-1}) in batch elution systems: (*a*) Leaching from Sc loaded am-TiP and (*b*) leaching from Fe(III)/Ca/Al-loaded am-TiP.

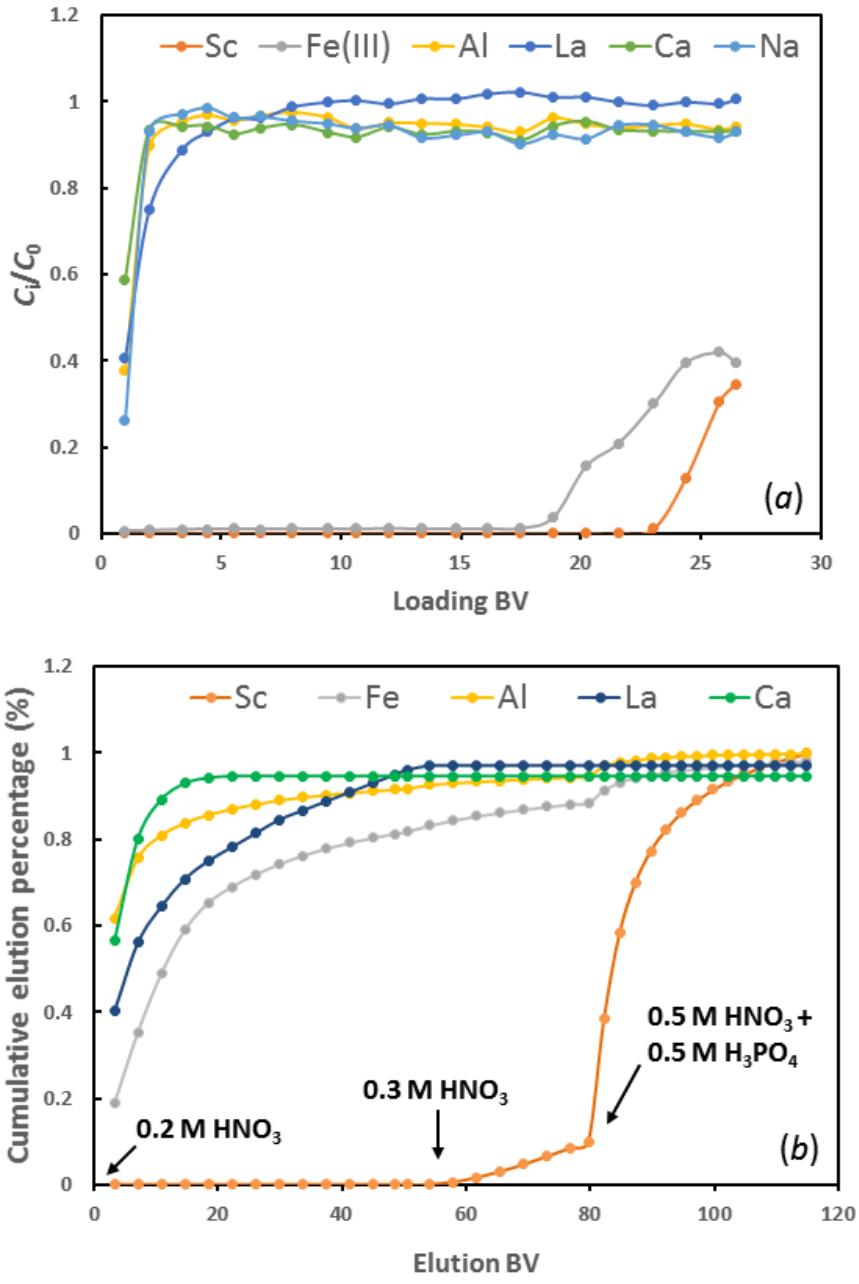

Figure 9. (*a*) Breakthrough of metal ions in simulated BR leachate at pH 2.0 on am-TiP column and (*b*) chromatographic elution of simulated BR leachate-load am-TiP column utilizing three different acid solutions.

Efficient and Selective Recovery of Trace Scandium by Inorganic Titanium Phosphate Ion-Exchangers from Leachates of Waste Bauxite Residue

Wenzhong Zhang*